# FINITE ELEMENT ANALYSIS OF A LINEAR ELASTIC MICROPOLAR CONTINUUM: APPLICATION OF QUADRILATERAL ELEMENTS IN 2D PROBLEMS

Sara Grbčić [1,2], Adnan Ibrahimbegović [2], Gordan Jelenić [1]

[1] University of Rijeka, Faculty of Civil Engineering, sara.grbcic@uniri.hr, gordan.jelenic@uniri.hr
[2] Université de Technologie de Compiègne / Sorbonne Universités, adnan.ibrahimbegovic@utc.fr

## 1. Introduction

The classical (Cauchy) continuum theory faithfully reproduces numerous experimental results carried out on many construction materials such as steel and aluminium. However, during experiments with polyurethane foam performed by Lakes [1] nonclassical size effects inconsistent with classical elasticity are observed that are describable by a Cosserat elastic model. Newer materials, such as materials with granular, fibrous or lattice structure cannot be adequately modelled by the classical theory, especially in such states of stress that show considerable stress gradients [2], for instance in the neighbourhood of holes, notches and cracks. Furthermore, experimental results show the presence of a size effect which is not taken into account in the classical continuum theory. The reason why materials act in an unexpected way according to Cauchy's predictions is that in those cases the influence of the microstructure is significant. In order to resolve these problems, a number of alternative continuum theories have been developed, including the so-called micropolar (Cosserat) theory where we presume the existence of an additional vector field which we call the moment stress vector as well as an independent microrotation field. Now, even when the volume of the body tends to zero, we can obtain moment vectors acting on the body. As a result the particle becomes orientable. Using this approach many new problems can be modelled, and the results obtained are much closer to the experimental results.

## 2. Micropolar continuum model

Let us analyse the body $\mathcal{B}$ of volume $V$ and surface $S$ in the deformed state under the influence of external actions consisting of distributed volume loads $\mathbf{p}_\mathrm{v}$ and $\mathbf{m}_\mathrm{v}$ and distributed surface loads $\mathbf{p}_\mathrm{s}$ and $\mathbf{m}_\mathrm{s}$, where $\mathbf{p}_\mathrm{v}$ is a specific body force, $\mathbf{m}_\mathrm{v}$ a specific body moment, $\mathbf{p}_\mathrm{s}$ a specific surface force and $\mathbf{m}_\mathrm{s}$ a specific surface moment. To generalise the Cauchy stress principle (see [3]), we consider an imaginary surface $S$ passing through an internal material point $X$ with the position $\mathbf{x}$ dividing the continuous body into two segments. One part of the body divided in this way will remain in equilibrium if, instead of the other part of the body, there exists a corresponding system of internal forces acting on the surface $S$. We presume the existence of a stress vector field $\mathbf{t}(\mathbf{x},t,\mathbf{n})$ and a couple-stress vector field $\mathbf{m}(\mathbf{x},t,\mathbf{n})$ acting on the infinitesimal surface $dS$ with a unit outward normal $\mathbf{n}$. According to the Cauchy principle, there exists a second-order tensor field $\boldsymbol{\sigma}(\mathbf{x},t)$ called the Cauchy stress tensor, which is independent of the outward normal $\mathbf{n}$ and describes the linear relationship between the force per unit area $\mathbf{t}(\mathbf{x},t,\mathbf{n})$ and $\mathbf{n}$, i.e. $\mathbf{t}(\mathbf{x},t,\mathbf{n}) = \boldsymbol{\sigma}(\mathbf{x},t)\,\mathbf{n}$. By generalising the Cauchy principle, we prove the linear relationship between the couple-stress vector $\mathbf{m}$ and the outward normal $\mathbf{n}$, and consequently obtain an additional, couple-stress tensor $\boldsymbol{\mu}(\mathbf{x},t)$ of order two, i.e. $\mathbf{m}(\mathbf{x},t,\mathbf{n}) = \boldsymbol{\mu}(\mathbf{x},t)\,\mathbf{n}$.

**Equilibrium equations.** We analyse a differential volume $dV$ in the deformed state and by summing all the components of the applied load and internal forces along the co-ordinate axes we obtain the force

equilibrium equation

$$\boldsymbol{\sigma}\nabla + \mathbf{p_v} = \mathbf{0}, \tag{1}$$

where $\nabla$ is the nabla differential operator, and the moment equilibrium equation

$$\boldsymbol{\mu}\nabla + \mathbf{a} + \mathbf{m_v} = \mathbf{0}, \tag{2}$$

where $\mathbf{a}$ is an axial vector of the double skew-symmetric part of the stress tensor, i.e.

$$\mathbf{a} = \text{axial}(2\boldsymbol{\sigma}_\text{a}) = \left\{\sigma_{32} - \sigma_{23} \quad -\sigma_{31} + \sigma_{13} \quad \sigma_{21} - \sigma_{12}\right\}^\text{T}, \tag{3}$$

both written in matrix form. By analysing the differential surface subject to surface loading we obtain the following boundary conditions:

$$\boldsymbol{\sigma}\ \mathbf{n} = \mathbf{p_s}, \qquad \boldsymbol{\mu}\ \mathbf{n} = \mathbf{m_s}. \tag{4}$$

**Kinematic equations.** We limit our attention only to linear analysis and derive the kinematic equations by analysing geometry of the deformation process. The detail of this approach can be found in [4]. In relation to the classical continuum theory, in the micropolar continuum theory we have an additional kinematic field $\boldsymbol{\varphi}(\mathbf{x})$ known as the microrotation field which represents the local rotation of the point $X$ and is completely independent of the displacement field. Consequently, it is important to note that the microrotation $\boldsymbol{\varphi}$ is completely independent and different from the rotational part $\boldsymbol{\Omega}$ of the displacement gradient, i.e. from the macrorotation $\boldsymbol{\omega}$ of the classical continuum theory (see [3]). The normal strains of the linear micropolar continuum $\epsilon_{ii}$ are defined as the change in length of a material fibre per initial length, when the initial length tends to zero. By analysing the body on a differential level we obtain

$$\epsilon_{ii} = \frac{\partial u_i}{\partial x_i} = \varepsilon_{ii},\ i = 1,2,3, \tag{5}$$

where $\varepsilon_{ii}$ is the normal strain in the classical continuum theory and $x_i$ are the Cartesian coordinates of $X$. We can see that the normal strains in the micropolar continuum theory are equal to those in the classical continuum theory, which means that the microrotation $\boldsymbol{\varphi}$ does not contribute to stretching or shortening of the generic fibre. The influence of the microrotation will become present in shear strains $\epsilon_{ij},\ i,j = 1,2,3,\ i \neq j$. A micropolar shear strain is defined to be equal to the difference of the change of inclination of a generic fibre during deformation and the microrotation $\boldsymbol{\varphi}$. By expanding the obtained functions into Taylor series and neglecting higher order terms we obtain

$$\epsilon_{ij} = u_{i,j} + \varepsilon_{kij}\varphi_k, \tag{6}$$

where $\varepsilon$ is the permutation tensor. Since we have an additional kinematic field $\boldsymbol{\varphi}(x_1,x_2,x_3)$, we should also define a corresponding angular strain which is a result of the existence of couple-stresses. For the planar deformation, for example, curvature $\kappa_{31}$ is defined as a change of rotation $\varphi_3(x_1,x_2)$, along axis $x_1$. The first index denotes the axis around which the rotation is taking place and the second index denotes the direction of change of the rotation. By expanding the obtained functions into Taylor series, we obtain

$$\boldsymbol{\kappa} = \text{grad}\ \boldsymbol{\varphi} = \boldsymbol{\varphi} \otimes \nabla. \tag{7}$$

Diagonal terms in $\boldsymbol{\kappa}$ represent torsional strains. The classical continuum theory is a special case of the micropolar continuum theory where the macrorotation vector $\boldsymbol{\omega}$ is equal to the microrotation vector $\boldsymbol{\varphi}$.

**Constitutive equations.** The most general relationship between two second-order tensors $\boldsymbol{\sigma}$ and $\boldsymbol{\varepsilon}$ is via a fourth-order tensor know as the constitutive tensor $\mathbf{T}$ which can be written in the component form as follows:

$$\sigma_{ij} = T_{ijpq}\varepsilon_{pq}, \tag{8}$$

where $i,j,p,q = 1,2,3$ are summational. We are analysing a linear, elastic and isotropic continuum, which means that the components of the constitutive tensor $\mathbf{T}$ remain unaffected by the orthogonal transformation. The most general fourth-order isotropic tensor $T_{ijpq}$ has the following form:

$$T_{ijpq} = \lambda\,\delta_{ij}\delta_{pq} + \mu(\delta_{ip}\delta_{jq} + \delta_{iq}\delta_{jp}) + \nu(\delta_{ip}\delta_{jq} - \delta_{iq}\delta_{jp}), \tag{9}$$

where $\lambda$, $\mu$, and $\nu$ represent the material parameters and have the same value in all coordinate systems and $\delta_{ij}$ is the Kronecker symbol. The proof is given in [5]. In the micropolar continuum theory we have two independent stress tensors $\boldsymbol{\sigma}$ and $\boldsymbol{\mu}$ related to two independent strain tensors $\epsilon$ and $\boldsymbol{\kappa}$. Both pairs of stress and strain tensors are non-symmetric. Thus, we have to obtain two fourth-order isotropic tensors with three independent material parameters each, which means that we will obtain six independent material constants in total. Constitutive equations of the micropolar continuum are defined as follows:

$$\sigma_{ij} = \lambda\,\epsilon_{pp}\delta_{ij} + (\mu+\nu)\epsilon_{ij} + (\mu-\nu)\epsilon_{ji}, \qquad \mu_{ij} = \gamma\kappa_{pp}\delta_{ij} + (\alpha+\beta)\kappa_{ij} + (\alpha-\beta)\kappa_{ji}, \tag{10}$$

where $\alpha$, $\beta$, $\gamma$, $\lambda$, $\mu$, $\nu$ represent the material parameters which describe the behaviour of the linear isotropic micropolar continuum.

## 3. Finite element formulation

To construct a numerical solution procedure of the boundary value problem analysed, we abandon its strong form (1)-(2) in favour of the weak form. The weak form is obtained by means of the principle of virtual work which states that virtual work of external and internal forces should remain the same, i.e.

$$G(\mathbf{u},\boldsymbol{\varphi};\overline{\mathbf{u}},\overline{\boldsymbol{\varphi}}) = G^{int}(\mathbf{u},\boldsymbol{\varphi};\overline{\mathbf{u}},\overline{\boldsymbol{\varphi}}) - G^{ext}(\overline{\mathbf{u}},\overline{\boldsymbol{\varphi}}) = \mathbf{0}. \tag{11}$$

Virtual work of internal and external forces is defined as

$$G^{int}(\mathbf{u},\boldsymbol{\varphi};\overline{\mathbf{u}},\overline{\boldsymbol{\varphi}}) = \int_V (\overline{\boldsymbol{\epsilon}}\cdot\boldsymbol{\sigma} + \overline{\boldsymbol{\kappa}}\cdot\boldsymbol{\mu})dV, \quad G^{ext}(\overline{\mathbf{u}},\overline{\boldsymbol{\varphi}}) = \int_V (\overline{\mathbf{u}}\cdot\boldsymbol{p_v} + \overline{\boldsymbol{\varphi}}\cdot\boldsymbol{m_v})dV + \int_S (\overline{\mathbf{u}}\cdot\boldsymbol{p_s} + \overline{\boldsymbol{\varphi}}\cdot\boldsymbol{m_s})dS, \tag{12}$$

where $\overline{\mathbf{u}}$ and $\overline{\boldsymbol{\varphi}}$ are the virtual displacements and virtual microrotation vectors, respectively, and $\overline{\boldsymbol{\epsilon}}$ and $\overline{\boldsymbol{\kappa}}$ represent the corresponding tensors of virtual strains and virtual curvatures.

**Displacement and microrotation field interpolation.** We construct the finite element approximation in a 2D domain and we choose a 4-node isoparametric quadrilateral element (Q4) to discretize the domain. The first choice of interpolation for $\mathbf{u}$, $\boldsymbol{\varphi}$, $\overline{\mathbf{u}}$ and $\overline{\boldsymbol{\varphi}}$ are the bilinear isoparametric shape function defined as follows:

$$\mathbf{u}^h(\xi,\eta) = \sum_{a=1}^{4} N_a(\xi,\eta)\,\mathbf{d_a}^e, \quad \text{where} \quad N_a(\xi,\eta) = \frac{1}{4}(1+\xi_a\xi)(1+\eta_a\eta);\ \xi_a = \pm 1,\ \eta_a = \pm 1;\ a = 1,2,3,4. \tag{13}$$

The same interpolation is used for $\boldsymbol{\varphi}$, $\overline{\mathbf{u}}$ and $\overline{\boldsymbol{\varphi}}$.

In order to satisfy the same order of the polynomial in the strain approximation (see equation (6)), an alternative interpolation is proposed, which is referred to as linked [6] or Allman-type [7] interpolation (Q4+LI) where the displacement approximation depends not only on nodal displacements, but also on microrotations, as follows:

$$\mathbf{u}^h(\xi,\eta) = \sum_{a=1}^{4} N_a(\xi,\eta)\,\mathbf{d_a}^e + \sum_{a=5}^{8} NS_a(\xi,\eta)\,\frac{l_{ij}}{8}(\varphi_j - \varphi_i)\mathbf{n}_{ij}, \tag{14}$$

where $l_{ij}$ and $\mathbf{n}_{ij}$ are the length and the outward unit normal vector, respectively, on the element side associated with the corner nodes $i$ and $j$, i.e.

$$\mathbf{n}_{ij} = \begin{Bmatrix} n_x \\ n_y \end{Bmatrix} = \begin{Bmatrix} \cos\alpha_{ij} \\ \sin\alpha_{ij} \end{Bmatrix}, \quad l_{ij} = \sqrt{(x_j - x_i)^2 + (y_j - y_i)^2}, \tag{15}$$

and $NS_a(\xi,\eta)$ are the serendipity-type shape functions defined as:

$$NS_a(\xi,\eta) = \frac{1}{2}(1-\xi^2)(1+\eta_a\eta), \quad a = 5,7, \qquad NS_a(\xi,\eta) = \frac{1}{2}(1+\xi_a\xi)(1-\eta^2), \quad a = 6,8. \tag{16}$$

The microrotation field is interpolated using the bilinear shape functions defined in equation (13), i.e.

$$\varphi^h(\xi,\eta) = \sum_{a=1}^{4} N_a(\xi,\eta)\,\varphi_a^e, \;\; a = 1,2,3,4. \tag{17}$$

After inserting the kinematic and constitutive equations (6), (7) and (10) and introducing the displacement and microrotation field approximations, we obtain the basic set of algebraic equation of the finite element method, i.e.

$$\mathbf{K}\,\mathbf{d} = \mathbf{f}; \quad \mathbf{K} = \mathop{\mathbb{A}}_{e=1}^{n_{elem}} \mathbf{K}^e; \quad \mathbf{f} = \mathop{\mathbb{A}}_{e=1}^{n_{elem}} \mathbf{f}^e, \tag{18}$$

where $\mathbb{A}$ stands for the finite-element assembly operator [8]. Numerical examples using these two different types of interpolations are shown in the next section.

# 4. Numerical examples - patch test

In order to assure the stability and convergence of a finite element, we have to observe its behaviour by performing the so-called patch test. It can be defined as a check if a patch of elements subject to a constant strain will reproduce exactly the constitutive behavior of the material and result in correct stresses when the element becomes infinitesimally small. In contrast to the classical (Cauchy) elasticity, in the micropolar (Cosserat) elasticity there exist certain difficulties in defining equilibrium states of constant strain because of the presence of the independent rotation field in the definition of strain (see equation (5)). An equilibrium state of constant strain is obtained when the displacements are varied linearly, the rotation field is constant and a constant body couple is applied. According to Providas [9], the patch test for Cosserat continuum should consist of three test defined in Table 1.

Satisfaction of Test 1 implies that the element is capable of producing the state of constant strain, where the strain tensor remains symmetric, which is equivalent to the behaviour corresponding to the classical (Cauchy) theory. By performing the Test 2 we obtain the state of constant strain with the non-symmetric strain tensor, i.e. $\epsilon_{12} \neq \epsilon_{21}$. In the first two tests the ability of the element to reproduce the state of constant curvature is not checked, since in both tests the components of curvature are equal to zero. This implies that another test has to be performed in order to completely validate the element. States of constant curvature are obtained from a linearly varying rotation field, which produces linear shear strain components with $\epsilon_{12} \neq \epsilon_{21}$. The patch test is performed by applying the boundary conditions along the boundary of the domain and the corresponding loading and then the obtained results at internal (non-prescribed) nodes are checked. A rectangular region $x \in [0, 0.12]$, $y \in [0, 0.24]$, covered by five arbitrarily distorted, non-overlapping quadrilateral elements is analysed, as shown in Figure 1. The chosen material parameters are equal to $\alpha + \beta = 40$, $\mu = 1000$, $\nu = 500$, $\lambda = 1000$.

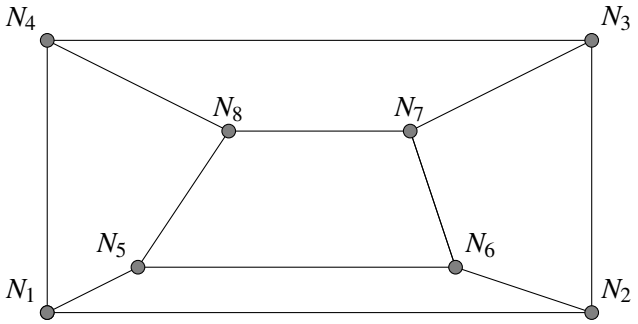


$N_1$ (0.00, 0.00) $N_5$ (0.04, 0.02)
$N_2$ (0.24, 0.00) $N_6$ (0.18, 0.02)
$N_3$ (0.24, 0.12) $N_7$ (0.16, 0.08)
$N_4$ (0.00, 0.12) $N_8$ (0.08, 0.08)

Figure 1: Finite element mesh for patch test

Table 1: Patch test: boundary conditions and loading [9]

| | | | |
|---|---|---|---|
| **Test 1:** | | | |
| $u = 10^{-3}(x+0.5y)$, | $v = 10^{-3}(x+y)$, | $\varphi = 0.25 \cdot 10^{-3}$, | $p_x = p_y = m = 0$, |
| **Test 2:** | | | |
| $u = 10^{-3}(x+0.5y)$, | $v = 10^{-3}(x+y)$, | $\varphi = 0.75 \cdot 10^{-3}$, | $p_x = p_y = 0,\ \ m = 1$, |
| **Test 3:** | | | |
| $u = 10^{-3}(x+0.5y)$, | $v = 10^{-3}(x+y)$, | $\varphi = 10^{-3}[0.25+(x+y)]$, | $p_x = p_y = 1,\ \ m = 2(x+y)$. |

Test 1 and 2 are completely satisfied for both (Q4 and Q4+LI) elements to the higher computer accuracy. The results for Test 3 are shown in Table 2 where it can be seen that elements do not reproduce the exact results, even though a relatively close agreement is achieved.

Table 2: Patch test, test 3: displacements at node $N5$ $(0.04, 0.02)$

| | $u \times 10^{-3}$ | $v \times 10^{-3}$ | $\varphi \times 10^{-3}$ |
|---|---|---|---|
| Q4 | 0.04992 | 0.060011 | 0.26095 |
| Q4+LI | 0.05025 | 0.063451 | 0.26192 |
| Exact | 0.05 | 0.06 | 0.27 |

# 5. Discussion

One of the ideas to enhance the element performance is by introducing the incompatible modes into the displacement interpolation. The quadrilateral membrane finite element with drilling degrees of freedom proposed in [10] is derived from variational principles employing an independent rotation field. Such element exhibits excellent accuracy characteristics, and in order to achieve that level of convergence for a micropolar finite element, one of the ideas is to modify the given functional in [10] by adding the contribution of the couple stresses and the independent behaviour of the microrotation field.

**Acknowledgement.** This work was supported by the Croatian Science Foundation Grant No. IP 1631 *Configuration-dependent approximation in non-linear finite-element analysis of structures* and by the French Embassy in Croatia through the French Government scholarship for doctoral level.

## References

[1] R.S. Lakes *Experimental microelasticity of two porous solids*, The International Journal of Solids and Structures, Vol. 22, pp. 55-63, 1986.

[2] W. Nowacki *Theory of micropolar elasticity*, Springer-Verlag, Vienna, 1972.

[3] L. E. Malvern *Introduction to the mechanics of a continuous medium*, Prentice-Hall, Inc, New Jersey, 1969.

[4] S. Grbčić *Micropolar elasticity - equilibrium, kinematic and constitutive equations*, seminar paper, subject: Applied Higher Mathematics, Rijeka, 2016.

[5] H. Jeffreys, B. Jeffreys *Methods of Mathematical Physics*, Cambridge University Press, Cambridge, 1956.

[6] D. Ribarić, G. Jelenić *Higher-order linked interpolation in quadrilateral thick plate finite elements*, Finite Elements in Analysis and Design, Vol. 51, pp. 67-80, 2012.

[7] D.J. Allman *The constant strain triangle with drilling rotations: A simple prospect for shell analysis*, Proceedings The Mathematics of Finite Elements and Applications, pp. 230-236, 1987.

[8] A. Ibrahimbegović *Nonlinear Solid Mechanics: Theoretical Formulations and Finite Element Solution Methods*, Springer, London, 2009.

[9] E. Providas, M.A. Kattis *Finite element method in plane Cosserat elasticity*, Computers and Structures Vol. 80, pp. 2059-2068, 2002.

[10] A. Ibrahimbegović, R. L. Taylor, E.L. Wilson *A robust quadrilateral membrane finite element with drilling degrees of freedom*, Internatonal journal for numerical methods in engineering, Vol. 30, pp. 445-457, 1990.